ACS APPLIED MATERIALS & INTERFACES

Research Article

www.acsami.org

Preparation of Microporous Silicone Rubber Membrane with Tunable Pore Size via Solvent Evaporation-Induced Phase Separation

Jian Zhao,[†] Gaoxing Luo,[‡] Jun Wu,[‡] and Hesheng Xia*,[†]

[†]State Key Laboratory of Polymer Materials Engineering, Polymer Research Institute of Sichuan University, Chengdu 610065, China

[‡]State Key Laboratory of Trauma, Burn and Combined Injury, Institute of Burn Research, Southwestern Hospital, Third Military Medical University, Chongqing 400038, China

Supporting Information

ABSTRACT: Silicone rubber membrane with ordered micropores in the surface was prepared by means of the solvent evaporation-induced phase separation. A ternary solution including liquid silicone rubber precursor, liquid paraffin, and hexane was cast to form a film with a two-phase structure after the hexane was evaporated. The micropores were generated by removing liquid paraffin phase in the cured silicone rubber film. The effects of the liquid paraffin concentration, casting temperature, initial casting solution thickness, air circulation, and addition of surfactant Span-80 on the pore structure in the membrane surface were investigated. The average pore size increases with increasing liquid paraffin concentration or the initial casting solution thickness. The formation of pore structure in the membrane surface is related to the phase separation and thus the phase separation process of the casting solution surface was in situ observed using the digital microscope. The formation mechanism of pore is attributed to a nucleation, growth, and coalescence process of liquid paraffin phase in the membrane surface.

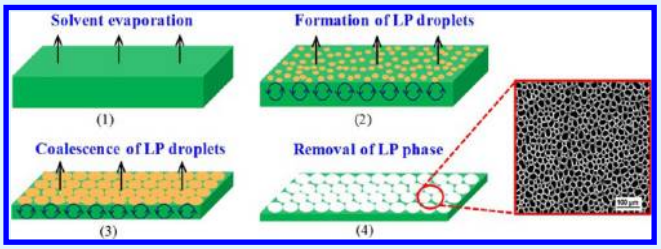

KEYWORDS: *microporous membrane, evaporation-induced phase separation, silicone rubber, liquid paraffin, phase diagram, surface morphology*

1. INTRODUCTION

Microporous polymer membrane have attracted much attention because of their wide applications in separation process,[1,2] tissue engineering,[3−6] drug-delivery systems,[7,8] catalysts,[9] photonic devices,[10] and microsieves.[11] One of the most promising strategies for the production of porous polymer membranes is the phase separation process.[12] The phase separation methods can be classified into four main methods: precipitation by cooling, called thermally induced phase separation (TIPS);[13] immersion precipitation (typically water), called nonsolvent-induced phase separation (NIPS);[14] precipitation by absorption of nonsolvent (water) from the vapor phase, called vapor induced phase separation (VIPS);[15] and solvent evaporation-induced phase separation, EIPS.[16]

For the EIPS method, a polymer is dissolved in a mixture of a volatile solvent and a less volatile nonsolvent. With the solvent evaporating, the nonsolvent enriched droplets grow and coalesce to be larger, the polymer solution is forced to separate into two phases: the polymer-rich phase and polymer-lean phase. Finally, the porous structure is formed by removing these nonsolvent enriched droplets.

The mechanism of phase separation for EIPS includes spinodal decomposition (SD) and nucleation and growth (NG) according to the composition change paths disclosed in the phase diagram. As shown in Figure 1, when the composition change path passes through the critical point (path 1), the phase separation occurs in the unstable region, the two-phase

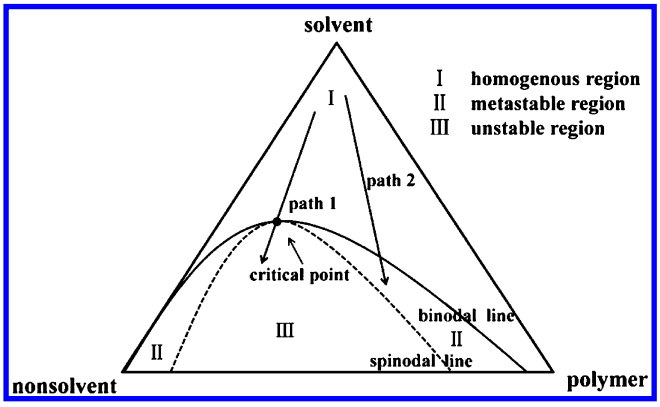

Figure 1. Ternary phase diagram for the polymer/solvent/nonsolvent system, in which the possible composition paths were marked.

structure forms through a SD mechanism. On the other hand, when the composition change path passes slowly in the metastable region (path 2), leading to nucleation and growth of the polymer-lean phase, the phase separation occurs through a NG mechanism. The phase morphology formed by the SD mechanism has a cocontinuous structure, whereas that formed

Received: December 2, 2012
Accepted: March 1, 2013
Published: March 1, 2013

by the NG mechanism has a cellular structure.[17,18] Besides, some factors such as the polymer concentration, type of solvent, membrane thickness, type and concentration of nonsolvent,[19,20] temperature, and air circulation[21] could also affect the phase morphology development and the pore formation in the membrane.

Silicone rubber possesses excellent properties such as chemical stability, hydrophobicity, transparency, significant gas permeability, nontoxicity, as well as good biocompatibility.[22] In particular, the good biocompatibility makes silicone rubber useful in the area of tissue engineering.[23] However, it is difficult to prepare the porous silicone rubber products through phase separation because of the insolubility of cross-linked silicone rubber in volatile organic solvents. So far, the generally used method to prepare the porous silicone membrane is foaming or solid particles leaching. Kobayashi et al.[24] developed porous membranes using hydrolization curing of silicone rubber in the presence of water or alcohol. The formation of the pores in the membrane was a result of hydrogen bubbles, which were produced in the reaction between the SiH and OH groups. Ratnasabapathy et al.[25] generated pores in cured silicone rubber via in situ chemical reactions. The water and CO_2 produced by the reaction of $NaHCO_3$ and HCl formed pores within the silicone rubber membranes. King et al.[26] prepared porous silicone rubber force sensitive resistors using sugar cube as porogen. The pores were formed after the sugar was dissolved in water. Fuller et al.[27] invented a method of making a silicone rubber having a structure adapted for growth of cells or living tissue using the inorganic salt as sacrificial filler to make pores. Although the porous silicone rubber materials were obtained, the controllability and uniformity of the pore size is still a challenge because of the difficulty in controlling the foaming process and the dispersion of solid particles in the system.

Herein, we presented a simple and low-cost method to prepare microporous silicone rubber membranes from a solution of silicone precursor, hexane, and liquid paraffin through a solvent evaporation-induced phase separation process. The effects of the liquid paraffin concentration, the addition of Span-80, casting temperature, membrane thickness, and air circulation on the average pore size and the density of pores were investigated. The formation mechanism of the surface porous structure was proposed based on in situ observation of membrane formation and the composition change path in the phase diagram.

2. EXPERIMENTAL SECTION

Materials. Liquid silicone rubber (LSR) was purchased from Shenzhen Kuwart Silicone Materials Co., Ltd. China (K-1008, two-part system A:B = 1:1). Hexane (boiling point: 68.7 °C), liquid paraffin (LP, C16~C20 saturated alkane), and Sorbitan monooleate (Span-80) were purchased from Kelong Factory of Chemical Engineering Reagent, Chengdu, China.

Phase Diagram. The phase diagram of the ternary polymer/nonsolvent/solvent system can be obtained through determining the cloud point by dropwise addition of nonsolvent and solvent alternatingly under continuous stirring. The cloud point was observed visually by sudden occurrence of turbidity upon nonsolvent addition and clearing of the mixture upon solvent addition.[18,20]

Preparation of the Porous Silicone Rubber Membrane. Porous silicone rubber membrane was prepared by the dry-cast technique. The LSR precursor/LP/hexane or LSR precursor/LP/hexane/Span-80 solutions was prepared in a beaker and was cast into a PTFE mold. Then the PTFE mold was kept in an oven allowing the hexane to evaporate. After 60 min, the membrane was cured 30 min at 100 °C. The obtained cured membrane was released from the PTFE mold, and immersed in hexane under 60 °C for 4 days to remove the liquid paraffin rich phase to form the pores. During this process, the solvent hexane was changed everyday. After that, the silicone rubber membrane was soaked into ethanol and deionized water, successively. The membrane was finally dried under ambient temperature. (see details in the experimental section of the Supporting Information)

Scanning Electron Microscopy (SEM) Observation. The surface morphologies of porous silicone rubber membrane were observed by a scanning electron microscope (SEM; Inspect F, Philips). The membranes specimen was cut into small pieces (3×3 mm^2) and were placed on the SEM stage, coated with gold–palladium under a vacuum atmosphere. The pores size and their surface density were measured through the image analysis software Image-Pro Plus.

Digital Microscopy Observation. The phase separation of LSR/LP/hexane (25/20/55) (w/w/w) ternary solution was in situ observed using a digital microscope (VHX-1000, KEYENCE, Japan). The solution was cast in a PTFE mold, and then were observed and recorded during the solvent evaporation. The focal distance was adjusted due to the shrinkage of the solution thickness during the observation.

3. RESULTS AND DISCUSSION

3.1. Phase Diagram. The ternary phase diagram for the system LSR/LP/hexane was shown in Figure 2 and the casting

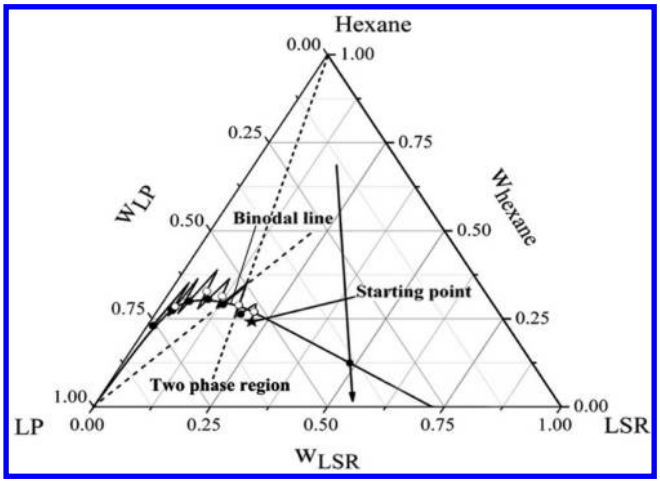

Figure 2. Phase diagram of LSR/LP/hexane system obtained by measuring could point, and the composition change path of the LSR/LP/hexane solution were marked.

solution composition change path during solvent evaporation was marked in the phase diagram. The phase diagram represents a detailed picture of the three components miscibility and it contains useful thermodynamic information about the phase separation process. The phase separation process due to solvent evaporation can be explained by the phase diagram. With the hexane evaporation occurring at the liquid/air interface, hexane concentration decreases to the critical value in the binodal line, the phase separation occurs initially at the liquid/air interface. With further evaporation of hexane, the phase separation occurs inside the solution.[28,29]

3.2. Pore Morphology. The uniformity of pore size and the density of pores in the surface of silicone membranes are dependent on the casting conditions, such as the liquid paraffin concentration, casting temperature, initial casting solution thickness, air circulation, and so on.

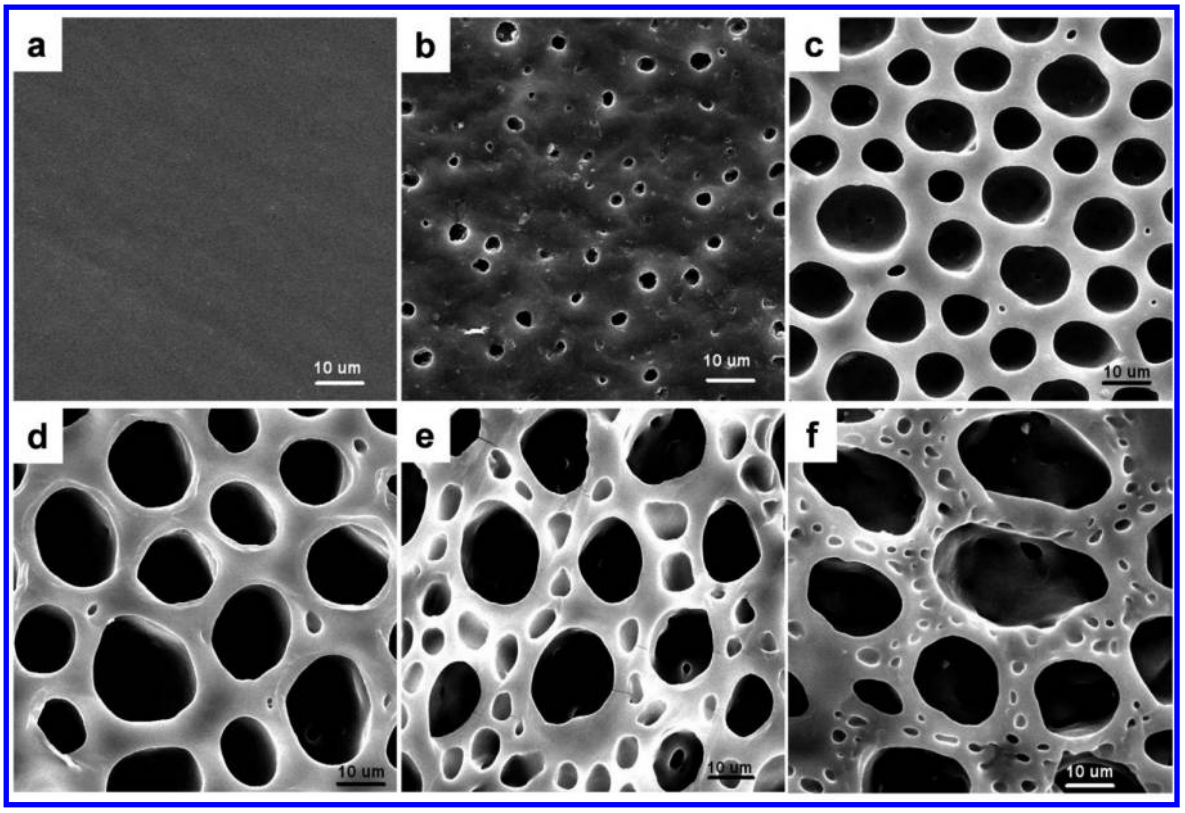

Figure 3. SEM micrographs of the surface morphologies of the porous silicone rubber membranes prepared at different liquid paraffin concentration: (a) 10, (b) 15, (c) 20, (d) 25, (e) 30, (f) 40 wt %.

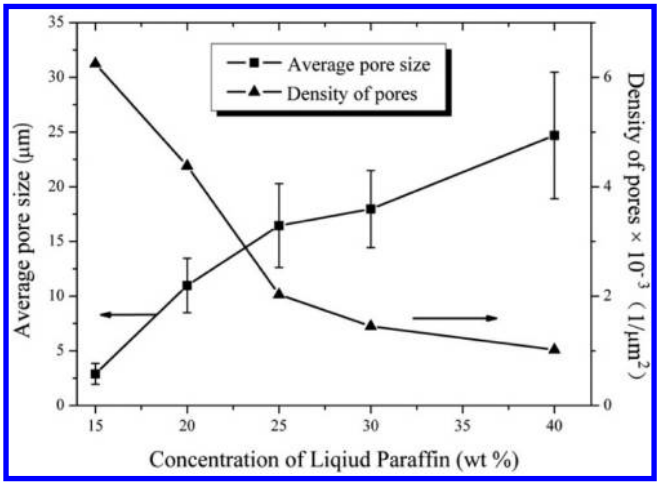

Figure 4. Average pore size and density of pores vs the concentration of liquid paraffin in casting solution.

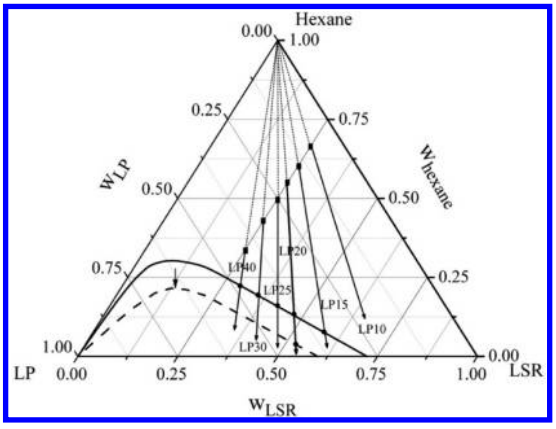

Figure 5. Composition change paths of solution containing different LP concentration during hexane evaporation process (■ denotes the initial solution composition, LP15 denotes composition change path for LSR/LP/hexane (25/15/60) (w/w/w) solution); The shifted binodal (dotted line) when increasing casting temperature or adding surfactant.

3.2.1. Effect of Liquid Paraffin Concentration on the Pore Structure. To investigate the effect of the concentration of LP on the uniformity of pore size and the density of pores on the membrane surface, various LSR/LP/hexane solutions with different LP concentration were applied, whereas the initial LSR concentration in the solution was set at 25 wt % and the initial casting solution thickness was 200 μm. Figure 3 shows SEM micrographs of surface morphologies of these membranes. The SEM images of different parts of the samples at lower magnification were shown in Figure S2 in the Supporting Information. The pores appears until the concentration of LP in the solution reaches 15 wt %. The average pore size and the density of pores on each membrane were measured from the SEM micrographs. The average pore size increases from ~2.90 to ~24.69 μm, and the density of pores decreases from ~6.25 × 10^{-3} to ~1.02 × 10^{-3} pore/μm^2 as the concentration of LP in the solution increases from 15 to 40 wt % (Figure 4). It also can be noted that the uniformity of the pore size decreases with the increase of LP concentration.

The effect of LP concentration on pore structures of the membrane can be qualitatively explained by the phase diagram. As shown in Figure 5, the composition change paths at different LP concentrations were marked in the phase diagram. The intersection point between composition change path and

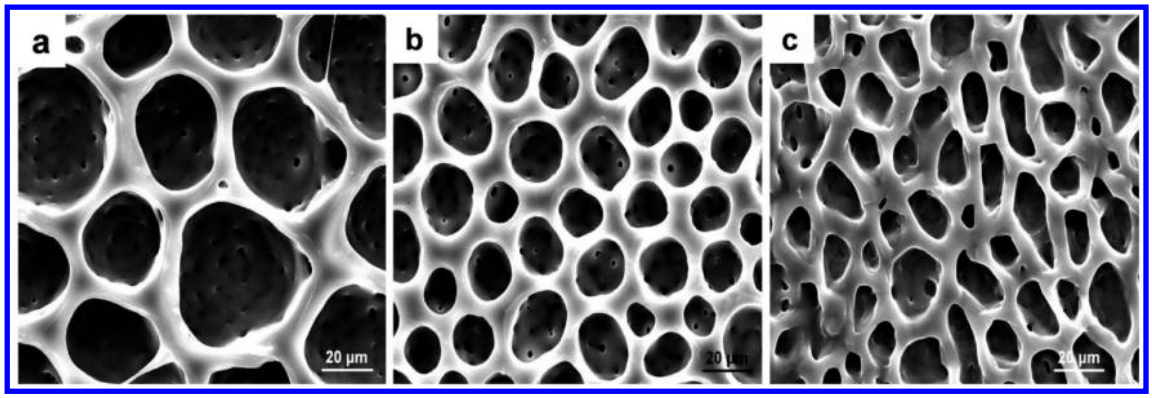

Figure 6. SEM micrographs of the surface morphologies of the porous silicone rubber membranes prepared at different casting temperatures: (a) 30, (b) 40, and (c) 50 °C.

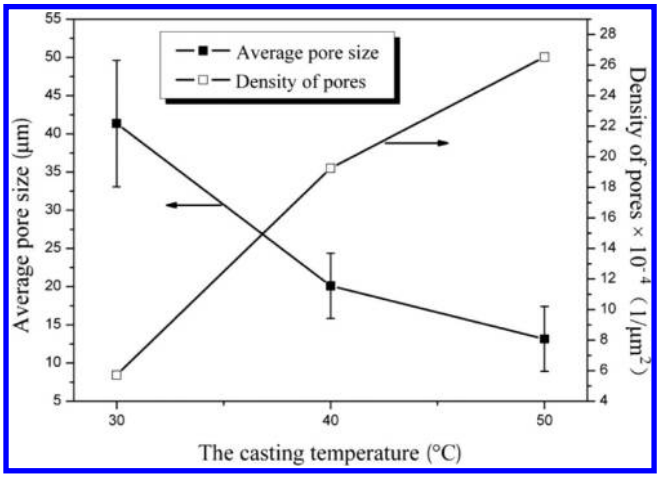

Figure 7. Average pore size and density of pores vs the casting temperature.

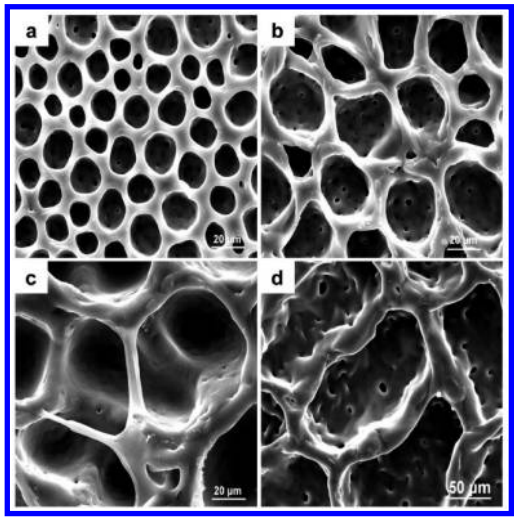

Figure 8. SEM micrographs of the surface morphologies of the porous silicone rubber membranes prepared with different initial casting solution thickness: about (a) 300, (b) 350, (c) 800, and (d) 1200 μm.

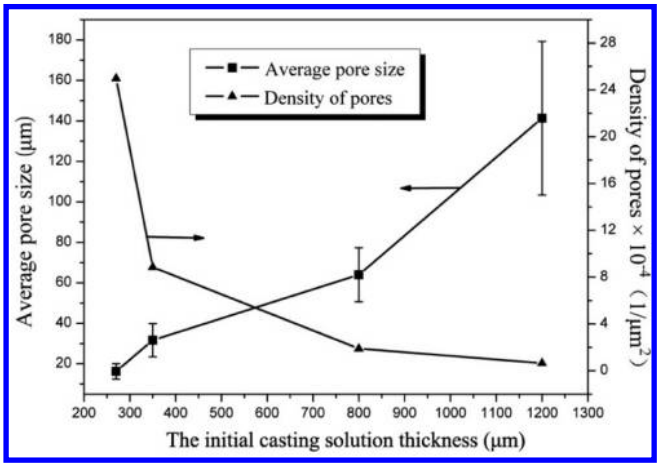

Figure 9. Average pore size and density of pores vs the initial casting solution thickness.

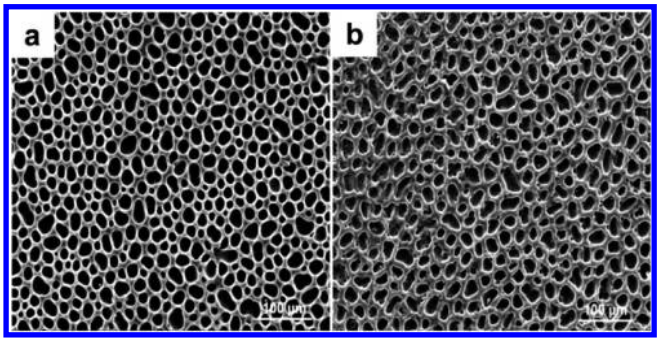

Figure 10. SEM micrographs of the surface morphologies of the porous silicone rubber membranes prepared (a) without and (b) with air circulation.

binodal curve represents the solution composition at the starting of phase separation. In the case of LP = 10 wt %, the composition change path does not cross the binodal line, the phase separation will not occur, which indicates that the small amount of nonpolar LP can disperse in the LSR in the form of molecules, consequently, no porous structures are obtained (Figure 3a). When the concentration of liquid paraffin increases to 15 wt %, the casting solution starts to undergo a process of phase separation, the composition change path crosses the binodal line during hexane evaporation. With increasing LP content, the LSR concentration at the point where composition change paths cross the binodal line decreases, the phase separation occurs at a higher solvent (hexane) concentration, in that case, the viscosity of solution at the onset of phase separation is lower. The lower viscosity of solution is beneficial to the growth and coalescence of the liquid paraffin rich

dx.doi.org/10.1021/am302929c | ACS Appl. Mater. Interfaces 2013, 5, 2040−2046

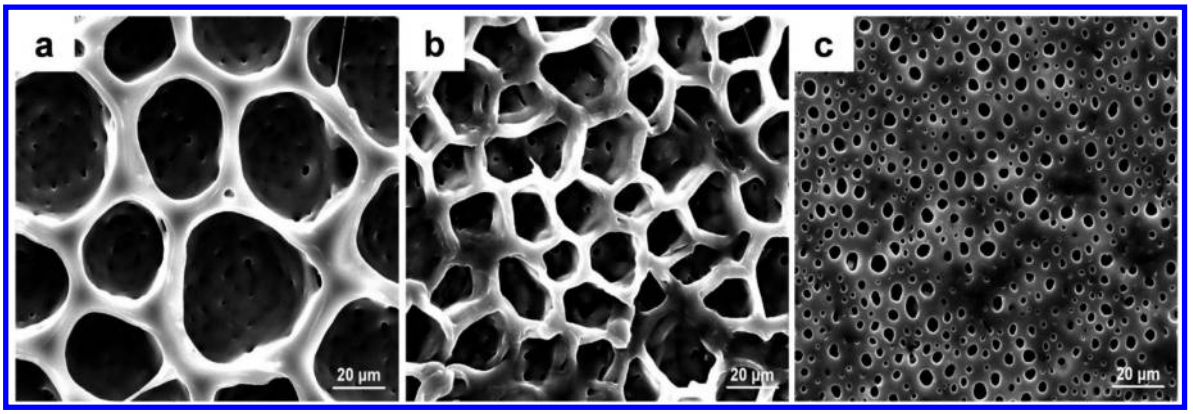

Figure 11. SEM micrographs of the surface morphologies of the porous silicone rubber membranes prepared from the cast LSR/LP/hexane (25/20/55)(w/w/w) solution with different content of Span-80: (a) 0, (b) 1, and (c) 2 phr.

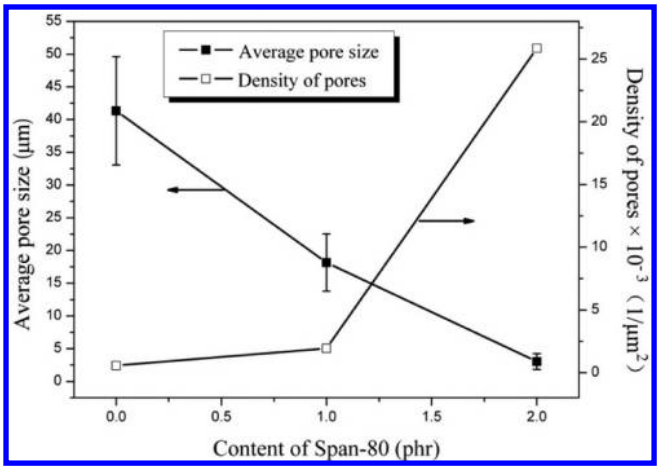

Figure 12. Average pore size and density of pores vs the content of Span-80 in casting solution.

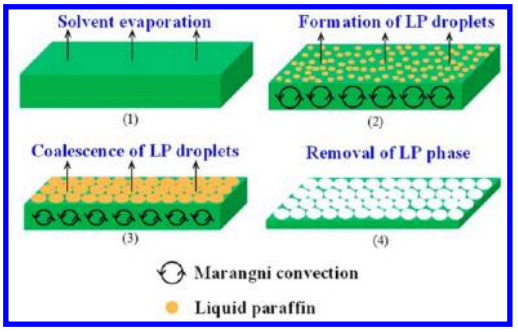

Figure 13. Schematic illustration for the pore formation process in the surface of silicone rubber membrane.

droplets. Thus, the pore size increases with increasing the LP concentration.

At 30 and 40 wt % LP, we can observe the presence of small pores on the big pore walls (Figure 3e, f). There are two reasons to explain this phenomenon. First, at a higher LP content, due to the low amount of hexane, phase separation in the solution occurs rapidly, some small LP-rich droplets do not coalesce before the solution demixes completely. Second, when the hexane evaporates, a portion of liquid paraffin dispersed in the polymer-rich phase, may undergo a second nucleation step to form the small pores at the later stage of the membrane formation process.

3.2.2. Effect of Casting Temperature on the Pore Structure. Figure 6 shows the surface morphologies of membranes prepared at different temperatures. When the casting temperature increases from 30 to 50 °C, the average pore size decreases from ~41.35 to ~15.09 μm, and the density of pores increases from ~5.72×10^{-4} to ~26.53×10^{-4} pore/μm^2 (Figure 7).

The effect of temperature on the phase separation process also can be explained by the phase diagram of this system. At a higher temperature the LSR solubility improves and the binodal line moves toward the higher LP concentration (Figure 5 dotted line). Therefore, the onset of phase separation moves toward the higher LSR concentration. Although the LSR/LP ratio is the same, the higher LSR concentration at the point where composition change path crosses the binodal line reduces the growth rate of the LP-rich droplets, and thereby smaller LP-rich droplets formed on the surface. In addition, hexane evaporates faster at a higher casting temperature, there is no enough time for the liquid paraffin rich droplets growing and coalescing. As a result, smaller pores are formed on the cured membrane surface at higher temperature.

3.2.3. Effect of Initial Casting Solution Thickness on the Pore Structure. The initial casting solution thickness also has influences on the pore structure. Four membranes with the initial casting solution thickness of 300, 350, 800, and 1200 μm were prepared. Figure 8 shows that the pore size is dependent on the initial casting solution thickness. As shown in Figure 9, the average pore size increases from ~16.25 to ~141.31 μm, and the density of pores decreases from ~24.97×10^{-4} to ~0.65×10^{-4} pore/μm^2 as the initial casting solution thickness increases from 300 to 1200 μm. Increasing the thickness results in an increase in the total mass of solvent, and a longer time is required for solvent evaporating completely, so there is adequate time for small LP-rich droplets to grow and coalesce larger during the phase separation.

3.2.4. Effect of Air Circulation during Evaporation Step on the Pore Structure. As illustrated in Figure 10, the membrane surface patterns become disordered and the average pore size decreases from ~20.09 to ~16.56 μm with the air circulation in the oven. The faster air flows, the hexane evaporates quickly, so the casting solution undergoes phase separation in a short time. The LSR rich phase shrinks making the final pores wall rough, and short time for the LP-rich droplets growing and coalescing leads to the formation of smaller pores on the surface. On the other hand, the air circulation on the surface will produce a

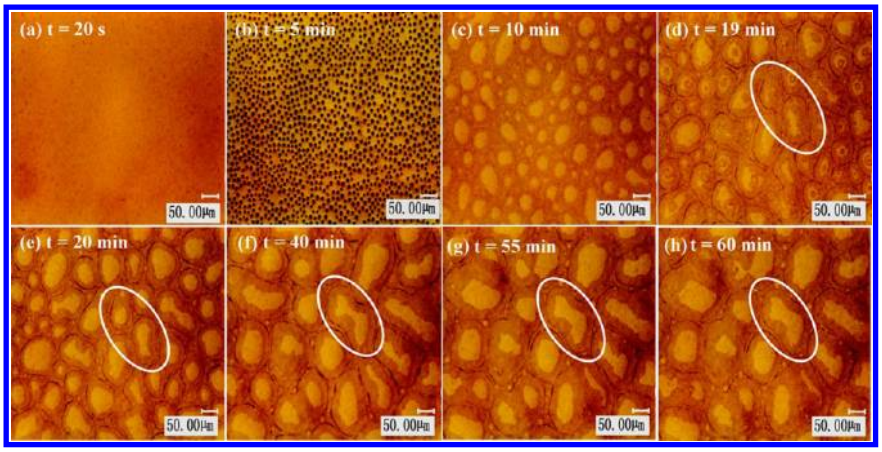

Figure 14. Evolution of liquid/air interface phase structure for the cast LSR/LP/hexane solution with a composition ratio (25/20/55) during solvent evaporation; t is the time from the onset of casting solution on the substrate. The initial casting solution thickness was 1200 μm.

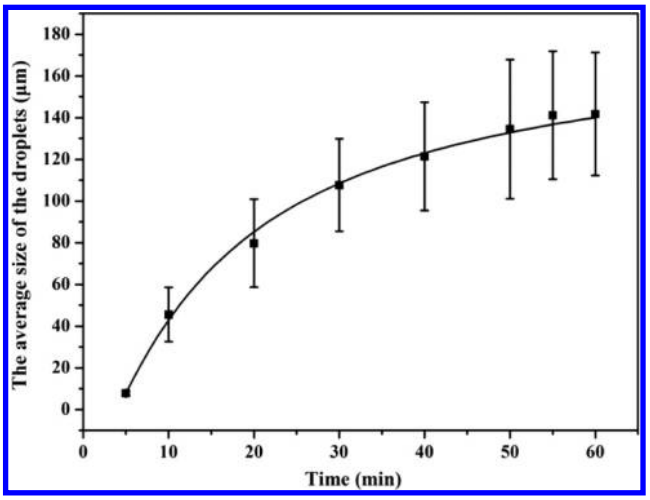

Figure 15. Average size of LP-rich droplets vs time; the size is evaluated from the optical images.

turbulent convection of liquid/air interface, consequently, the LP-rich droplets will form a disordered array.

3.2.5. Effect of Addition of Surfactant Span-80 on the Pore Structure. The effect of surfactant Span-80 in casting solution on the membrane surface pore size was investigated. Figure 11 shows the SEM micrographs of silicone rubber membranes prepared from the cast LSR/LP/hexane (25/20/55)(w/w/w) solution with different contents of Span-80. The average pore size decreases significantly from ~41.35 to ~3.03 μm, and the density of pores increases from ~0.57×10^{-3} to ~25.86×10^{-3} pore/μm^2 as the content of Span-80 increases from 0 to 2 phr (Figure 12). It should be noted that the addition of Span-80 significantly decreases the pore size. Span-80 as a nonionic surfactant can dissolve in the LSR/LP/hexane system, and the coalescence of LP-rich droplets in the liquid/air interface is hampered due to the decrease in the surface tension with surfactant. Also, the addition of Span-80 will possibly reduce the interfacial tension between LP-rich droplets and LSR, and improve the compatibility of LP and LSR, the phase separation will occur at a relatively higher LSR concentration (dotted line in Figure 5), so smaller LP-rich droplets are formed. On the other hand, the surfactant forms a protective layer at the surface of the droplets, preventing the mass transport across the interface, and thus hinders the growth of the droplets. Greenberg et al.[30] studied the effect of surfactant Triton X-100 on the formation of CA/acetone/water membrane. They found that the addition of surfactant reduces the surface tension gradients at the nonsolvent rich phase surface and thereby weakens the Marangni convection. This in turn reduces the mass-transfer and leads to the decrease in the size of non-solvent-rich phase.

3.3. Formation Mechanism of Pores in the Surface of Membrane. On the basis of the pore structure in the surface of membrane and the solution composition change path in the phase diagram during solvent evaporation (Figure 5), it is reasonable to conclude that the formation mechanism of pore is attributed to a nucleation, growth and coalescence process of liquid paraffin phase in the membrane surface. The formation process of porous in the surface of membrane can be divided into four steps (Figure 13): (1) evaporation of solvent; (2) formation of LP-rich droplets; (3) growth and coalescence of LP-rich droplets; (4) removal of LP-rich phase. With the solvent diffusing upward and evaporating, the phase separation starts to occur at the liquid/air interface and leads to the formation of small LP-rich droplets. The solvent evaporation rapidly cools the casting solution surface,[31] and produces the temperature gradient ΔT between the upper and bottom of the solution, which leads to the occurrence of Marangni convection.[32] The upflow and downflow of materials driven by convection enhances the mass transfer of LP into the growing LP-rich droplets. In the liquid/air interface, the interfacial tension-driven coalescence of the LP-rich droplets will occur to produce the bigger LP droplets during the solvent evaporation. If in the presence of the surfactant such as Span-80, interfacial tension decreases and the coalescence of LP droplets will be reduced . After removing the LP phase from cured silicone rubber membrane, the porous membrane surface is obtained. The two-phase structures formed by the phase separation are the prototype of pore structures.

To confirm the above formation mechanism, the formation process of LSR/LP/hexane (25/20/55) ternary solution surface was in situ observed using a digital microscope. Figure 14 shows temporal change in the pattern of the casting solution surface during the solvent evaporation. The nucleation, growth and coalescence of LP-rich droplets can be seen in these images. After casting the solution on the substrate, the solvent evaporates from the liquid/air interface, causing the increase of polymer concentration at the interface. The solution is homogeneous without demixing until the polymer concen-

tration increases to a critical value (Figure 14a). At $t \approx 5$ min, uniformly distributed spherical particles with an average size of ~7.79 μm appear (Figure 14b). They are considered to be the LP-rich droplets formed through phase separation. With solvent evaporating continuously, at $t \approx 55$ min, the LP-rich droplet size increases from ~7.79 to ~141.15 μm because of the coalescence of small droplets in the liquid/air interface (Figure 14g). From Figure 14d it can be observed that small liquid paraffin spheres (gray color) are temporarily coagulated on the big droplets (white color) before the complete coalescence, more evidence can be found in Figure S3 in the Supporting Information. After $t \approx 55$ min, the sizes of droplets increase no longer, which indicates that the droplets stop growing and coalescing, and the phase separation process is completed. The structure of LP-rich droplets shown in Figure 14h is similar to pore structure in the surface of the cured membrane (Figure 8d). Figure 15 shows that the average size of LP-rich droplets increases with time until the phase separation process is finished.

4. CONCLUSIONS

The evaporation-induced phase separation technique is a suitable, inexpensive and simple method to prepare porous silicone rubber membranes. The obtained membranes have an ordered pore structure and the average pore sizes are tunable. As the LP concentration increases, the membrane structure changes from entirely dense to porous. That is because the phase separation process does not occur at a low LP concentration. The average pore size in the membrane surface increases with increasing the concentration of LP in the solution. Moreover, the addition of Span-80 has significant influence on the membrane porous structure, and the average pore size decreases remarkably from ~41.35 to ~3.03 μm with 2 phr Span-80. The formation mechanism of porous structure in the surface of the membrane is considered to be a nucleation, growth and coalescence process. The prepared microporous silicone rubber membrane has a potential application in biomedical field such as artificial skin and scaffold for tissue engineering.

■ ASSOCIATED CONTENT

Supporting Information

Detailed experimental section, the pore morphologies at lower magnifications, and the coalescence of LP droplets. This material is available free of charge via the Internet at http://pubs.acs.org.

■ AUTHOR INFORMATION

Corresponding Author

*E-mail: xiahs@scu.edu.cn; Fax: +86 028 8546 0535; Tel: +86 028 8546 0535.

Notes

The authors declare no competing financial interest.

■ ACKNOWLEDGMENTS

This work was supported by National High-Tech Research and Development Program of China (863 Program 2012AA020504) and M12·5-AWS11J012-05.

■ REFERENCES

(1) Pinnau, I.; Koros, W. J. *J. Membr. Sci.* **1992**, *71* (1−2), 81−96.
(2) Ismail, A. F.; Yean, L. P. *J. Appl. Polym. Sci.* **2003**, *88*, 442−451.
(3) George, J.; Onodera, J.; Miyata, T. *J. Biomed. Mater. Res. A* **2008**, *87A*, 1103−1111.
(4) Fukazawa, H.; Hiromichi, K.; Fujinomiya. *Gas-exchange membrane for an artificial lung*. U.S. Patent 4 909 989, March 20, 1990.
(5) Cameron, N. R. *Polymer* **2005**, *46*, 1439−1449.
(6) Madihally, S. V.; Matthew, H. W. T. *Biomaterials* **1999**, *20*, 1133−1142.
(7) Herbig, S. H.; Carinal, J. R.; Korsmeyer, R. W.; Smith, K. L. *J. Controlled Release* **1995**, *35*, 127−136.
(8) Witte van de, P.; Esselbrugge, H.; Feijen, J. *J. Controlled Release* **1993**, *24*, 61−78.
(9) Davis, M. E. *Nature* **2002**, *417*, 813−821.
(10) Xia, Y. N.; Gates, B.; Yin, Y. D.; Lu, Y. *Adv. Mater.* **2000**, *12*, 693−713.
(11) Yan, F.; Ding, A.; Goedel, W. A. *Adv. Mater.* **2012**, *24*, 1551−1557.
(12) Ulbricht, M. *Polymer* **2006**, *47*, 2217−2262.
(13) Yave, W.; Quijada, R.; Ulbricht, M.; Benavente, R. *Polymer* **2005**, *46*, 11582−11590.
(14) Stropnik, C.; Musil, V.; Brumen, M. *Polymer* **2000**, *41*, 9227−9237.
(15) Bikel, M. *ACS Appl. Mater. Interfaces* **2009**, *1*, 2856−2861.
(16) Kim, J. K.; Taki, K.; Ohshima, M. *Langmuir* **2007**, *23*, 12397−12405.
(17) Nunes, S. P.; Inoue, T. *J. Membr. Sci.* **1996**, *111*, 93−103.
(18) Matsuyama, H.; Nishiguchi, M.; Kitamura, Y. *J. Appl. Polym. Sci.* **2000**, *77*, 776−782.
(19) Matsuyama, H.; Teramoto, M.; Uesaka, T. *J. Membr. Sci.* **1997**, *135*, 271−288.
(20) Jansen, J. C.; Macchione, M.; Drioli, E. *J. Membr. Sci.* **2005**, *255*, 167−180.
(21) Macchione, M.; Jansen, J. C.; Drioli, E. *Desalination* **2006**, *192*, 132−141.
(22) Mcdonald, J. C.; Whitesides, G. M. *Acc. Chem. Res.* **2002**, *35*, 491−499.
(23) Murphy, W. L.; Dennis, R. G.; Kileny, J. L.; Mooney, D. *Tissue Eng.* **2002**, *8*, 43−52.
(24) Wang, H. Y.; Kobayashi, T.; Saitoh, H.; Fujii, N. *J. Appl. Polym. Sci.* **1996**, *60*, 2339−2346.
(25) Jiao, K. X.; Graham, C. L.; Wolff, J. *J. Membr. Sci.* **2012**, *401−402*, 25−32.
(26) King, M. G.; Baragwanath, A. J.; Rosamond, M. C.; Wood, D.; Gallant, A. *Procedia Chem.* **2009**, *1*, 568−571.
(27) Fuller, J. P.; Pegg, D.; Bird, R. M.; Clifford, T. B.; Clayson, T. *Preparation of porous silicone rubber for growing cells or living tissue*. U.S. Patent 6 900 055 B1, May 31, 2005.
(28) Altinkaya, S. A.; Ozbas, B. *J. Membr. Sci.* **2004**, *230*, 71−89.
(29) Shojaie, S. S.; Krantz, W. B.; Greenberg, A. R. *J. Membr. Sci.* **1994**, *94*, 281−298.
(30) Khare, V. P.; Greenberg, A. R.; Zartman, J.; Krantz, W. B.; Todd, P. *Desalination* **2002**, *145*, 17−23.
(31) Srinivasarao, M.; Collings, D.; Philips, A.; Patel, S. *Science* **2001**, *292*, 79−83.
(32) Sakurai, S.; Furukawa, C.; Okutsu, A.; Miyoshi, A.; Nomura, S. *Polymer* **2002**, *43*, 3359−3364.